154 *J. Chem. Eng. Data* **1987**, *32*, 154-157

Thermodynamics of Protonation of *m*- and *p*-Nitroanilines in Water–Acetonitrile and Water–Dimethylformamide Mixtures

S. Subramanian, V. V. Giridhar, and C. Kalidas*

Department of Chemistry, Indian Institute of Technology, Madras 600 036, India

The thermodynamic dissociation constants (pK_a) of *m*-nitroanilinium ion ($mNAH^+$) in water–acetonitrile (AN) and water–dimethylformamide (DMF) mixtures and of *p*-nitroanilinium ion ($pNAH^+$) in water–DMF mixtures have been determined by a spectrophotometric method a 30 °C in various solvent compositions. While the pK_a of $mNAH^+$ ion in water–AN mixtures passed through a minimum at 60 wt % AN, that of $mNAH^+$ and $pNAH^+$ ions in water–DMF mixtures passed through a minimum at 80 wt % DMF. The solvent effect on the dissociation equilibria has been discussed, along with the available pK_a data on $pNAH^+$ in water–AN mixtures, in terms of the variation of transfer free energies of the various species involved in the equilibria.

Introduction

The variation of pK's of weak acids and bases in mixed solvents provides valuable information toward an understanding of solute–solvent interactions in these media (*1–4*). Although many investigations of this nature have been made in binary mixtures of aqueous–amphiprotic solvents, very few studies involving a dipolar aprotic solvent as one of the components have been reported hitherto. In continuation of our earlier work on this subject (*2*, *5–7*) the present paper, therefore, deals with the study of the solvent effect on the dissociation of *m*- and *p*-nitroanilinium ions in water–AN and water–DMF mixtures using a spectrophotometric method.

Experimental Section

Acetonitrile (S. Merck, India), DMF (E. Merck, India), and water were purified as described earlier (*8*, *9*). The indicators, *m*- and *p*-nitroaniline (Sisco Research Laboratories, India), were recrystallized twice from aqueous ethanol and their melting points (114 °C for mNA and 148 °C for pNA) were found to be in agreement with the reported (*10*) values. HCl gas, generated by adding concentrated H_2SO_4 to concentrated AR HCl, was purified as described earlier (*11*) and bubbled into the solvent mixture of desired composition. The strength of the stock acid solution was determined by titration against aqueous sodium hydroxide solution which was standardized previously by using a standard solution of potassium hydrogen phthalate. No perceptible change in the strength of the acid in various solvent mixtures was observed during the period of measurements in all compositions. The dissociation constants (pK_{BH^+}) of *m*- and *p*-nitroanilinium ions were determined spectrophotometrically in accordance with the procedure described earlier (*11*). The indicator ratio, m_{BH^+}/m_B, necessary for the evaluation of the dissociation constant was calculated (*12*) from

$$\frac{m_{BH^+}}{m_B} = \frac{E_B - E}{E - E_{BH^+}} \qquad (1)$$

where E, E_B, and E_{BH^+} represent the molar extinction coefficients of the experimental solution, of the basic form B, and of its protonated form BH^+. Absorbance measurements were carried out at 30 ± 0.1 °C by means of PMQ II Carl Zeiss spectrophotometer at the wavelength of maximum absorption of the basic form of the indicator in each solvent composition. E_{BH^+} was found to be negligibly small at this wavelength in all compositions. The solubilities of *m*- and *p*-nitroanilines were determined in the usual way as described earlier (*5*). The solubility measurements were repeated at least twice independently to check the reproducibility and the agreement between duplicates was better than ±1%. The pK_{BH^+} data of $pNAH^+$ upto 75 wt % AN at 25 °C, reported by El-Harakany et al. (*13*), were also analyzed to understand the solvent effect on this equilibrium, and the required solubility data were determined at 25 ± 0.1 °C. In the case of *m*-nitroaniline in water–AN mixtures, solubility measurements in the composition range between 30 and 80 wt % AN could not be performed due to the phase separation of the two solvent layers with the addition of mNA. No such difficulty was encountered below 30 wt % and above 80 wt % AN. Further experimental details are given elsewhere (*11*).

Results and Discussion

The pK_{BH^+} of *m*- and *p*-nitroanilinium ions (BH^+) according to the equilibrium

$$BH^+ \rightleftarrows B + H^+ \qquad (2)$$

was obtained by extrapolation of the plots of pK'_{BH^+} against the concentration, m, of the acid to $m \rightarrow 0$ in the various solvent mixtures. The function pK'_{BH^+} is defined by

$$pK'_{BH^+} = \log m_{BH^+}/m_B - \log m_{H^+} = pK_{BH^+} + f(m) \qquad (3)$$

where m_{H^+} represents the molal concentration of free hydrogen ions which is assumed to be equal to the stoichiometric concentration of the acid in the solution. In the case of mNA a correction was made (*14*) for the concentration of HCl at equilibrium taking BH^+ formed into consideration. The plots of pK'_{BH^+} vs. m were found to be fairly linear in all solvent compositions. In the calculation of pK'_{BH^+}, the acid was assumed to be completely dissociated in all solvent compositions, except in pure DMF. In this case, a correction was made for the ion association of HCl, using the association constant data available in pure DMF. Due to the instability of HCl in pure AN, pK_{BH^+} measurements were not performed in pure AN. The pK_{BH^+} of $mNAH^+$ and $pNAH^+$ ions in pure water at 30 °C are 2.42 and 0.99, respectively, which are in good agreement with the reported values (*15*, *16*) at the same temperature. The pK_{BH^+} data of $mNAH^+$ and $pNAH^+$, the solubilities, and Gibbs transfer energies, $\Delta G^\circ_{t(B)}$, of mNA and pNA (calculated from solubility data as described earlier (*5*)) in water–AN and water–DMF mixtures are given in Tables I and II.

A better insight into the variation of the pK_{BH^+} with solvent composition can be obtained by considering the variation of the transfer parameters of the equilibrium process (eq 2) with the solvent composition. The change of standard free energy associated with the dissociation equilibrium of BH^+ in the solvent (ΔG°_s) relative to that in pure water (ΔG°_w) may be related to the pK_{BH^+} difference of the indicator between the solvent under

0021-9568/87/1732-0154$01.50/0

Table I. pK_{BH^+} of mNAH$^+$ Ion (Molal Scale) and pK_{BH^+}, Solubility, and Transfer Free Energy Data of *m*-Nitroaniline in Water–AN and Water–DMF Mixtures at 30 °C

	water–AN mixtures				water–DMF mixtures			
wt % of org solvent component	pK_{BH^+}[a]	ΔpK_{BH^+}	solubility of mNA/mol kg^{-1}	$\Delta G°_{t(mNA)}$[b]/ kJ mol^{-1}	pK_{BH^+}[a]	ΔpK_{BH^+}	solubility of mNA/mol kg^{-1}	$\Delta G°_{t(mNA)}$[b]/ kJ mol^{-1}
0	2.42	0	7.744×10^{-3}	0	2.42	0	7.744×10^{-3}	0
20	1.88	−0.54	6.516×10^{-2}	−5.36	1.74	−0.68	0.03643	−3.90
30			0.181	−7.95				
40	1.52	−0.90			1.24	−1.18	0.1457	−7.40
60	1.30	−1.12			0.53	−1.89	0.9117	−12.02
80	1.40	−1.02	1.960	−13.93	0.06	−2.36	2.535	−14.60
90			2.279	−14.31				
100			2.377	−14.43	1.95	−0.47	3.192	−15.18

[a] Values accurate to ±0.01 unit. [b] Accurate to ±0.05 kJ mol^{-1}. Solubility values accurate to within ±1%.

Table II. pK_{BH^+} of pNAH$^+$ Ion (Molal Scale) and pK_{BH^+}, Solubility, and Transfer Free Energy Data of *p*-Nitroaniline in Water–AN (at 25 °C) and in Water–DMF (at 30 °C) Mixtures

	water–AN mixtures				water–DMF mixtures			
wt % of org solvent component	pK_{BH^+}[a]	ΔpK_{BH^+}	solubility of pNA/mol kg^{-1}	$\Delta G°_{t(pNA)}$[b]/ kJ mol^{-1}	pK_{BH^+}[c]	pK_{BH^+}	solubility of pNA/mol kg^{-1}	$\Delta G°_{t(pNA)}$[b]/ kJ mol^{-1}
0	1.02	0	4.379×10^{-3}	0	0.99	0	5.987×10^{-3}	0
20	0.46	−0.56	4.101×10^{-2}	−5.56	0.36	−0.63	0.03406	−4.38
40	0.04	−0.98	0.256	−10.08	−0.26	−1.25	0.1784	−8.56
60	−0.19	−1.21	0.691	−12.55	−0.88	−1.87	1.0624	−13.05
75	−0.30	−1.32	1.090	−13.68				
80					−1.75	−2.74	2.6335	−15.34
100					0.15	−0.84	4.025	−16.41

[a] Values from ref *13* interpolated at the compositions mentioned. [b] Values accurate to ±0.05 kJ mol^{-1}. [c] Values accurate to ±0.01 units. Solubilities accurate to within ±1%.

Table III. Thermodynamic Parameters (kJ mol^{-1}) of Various Species Involving mNA in Water–AN Mixtures at 30 °C (Molal Scale)

wt % AN	$\Delta G°_{t(B)}$[e]	$\Delta G°_{t(diss)}$[e]	$\Delta G°_{t(HCl)}$[b]	$\Delta G°_{t(Cl^-)}$[c]	$\Delta G°_{t(H^+)}$[d]	$\Delta G°_{t(BH^+)}$	$\Delta G°_{t(BHCl)}$	$\Delta G°_{t(B)} - \Delta G°_{t(BHCl)}$
0	0	0	0	0	0	0	0	0
20	−5.36	−3.13	1.25	1.79 (3.86)	−0.54 (−1.61)	−2.77 (−4.84)	−0.98	−4.38
30	−7.95	−4.30[a]	2.21	2.60 (5.60)	−0.39 (−3.39)	−4.04 (−7.04)	−1.44	−6.51
40		−5.22	3.45	3.68 (7.06)	−0.23 (−3.61)			
60		−6.50	7.02	6.40 (9.90)	0.62 (−2.88)			
80	−13.93	−5.92	14.64	12.16 (15.78)	2.48 (−1.14)	−5.53 (−9.15)	6.63	−10.56

[a] Interpolated from a large-scale plot of $\Delta G°_{t(diss)}$ vs. composition of AN. [b] By EMF method; ref *22*. [c] By nLJP method, using the relation $\Delta G°_{t(Cl^-)} = \Delta G°_{t(AgCl)} - \Delta G°_{t(Ag^+)}$; $\Delta G°_{t(AgCl)}$ from ref *21* and $\Delta G°_{t(Ag^+)}$ from ref *22*. Values in parentheses are based on the TATB method. [d] $\Delta G°_{t(H^+)} = \Delta G°_{t(HCl)} - \Delta G°_{t(Cl^-)}$. [e] Accurate to ±0.05 kJ mol^{-1}.

consideration and the reference solvent (water in the present case) by the expression

$$\Delta G°_{t(diss)} = 2.303RT\Delta pK_{BH^+} = \Delta G°_{t(H^+)} + \Delta G°_{t(B)} - \Delta G°_{t(BH^+)} \quad (4)$$

which can also be written as

$$\Delta G°_{t(diss)} = 2.303RT\Delta pK_{BH^+} = \Delta G°_{t(HCl)} + \Delta G°_{t(B)} - \Delta G°_{t(BHCl)} \quad (5)$$

The $\Delta G°_{t(i)}$, where i = B, BH$^+$, H$^+$ etc., in the above equations represents the Gibbs transfer energies of the species i from water to the solvent under consideration. The values of $\Delta G°_{t(BH^+)}$ and $\Delta G°_{t(BHCl)}$ were evaluated from eq 4 and 5 using the available transfer energy data of other species (see footnote under Tables III–VI). The thermodynamic quantities of the various species involved in the dissociation equilibria are recorded for mNAH$^+$ ion (Tables III and IV) and pNAH$^+$ ion (Tables V and VI).

It is seen that $\Delta G°_{t(diss)}$ for mNAH$^+$ and pNAH$^+$ ions in both the solvent mixtures over the entire range of solvent compositions is negative and thus the equilibrium is more favored in the mixed solvent than in pure water. The minimum observed in $\Delta G°_{t(diss)}$ can be explained as arising from the opposite variation of two factors, $\Delta G°_{t(HCl)}$ which is positive and continuously increases and $\Delta G°_{t(B)} - \Delta G°_{t(BHCl)}$ which is negative and continuously decreases with the addition of the organic component in both the solvent mixtures, the dominating factor being $\Delta G°_{t(B)} - \Delta G°_{t(BHCl)}$.

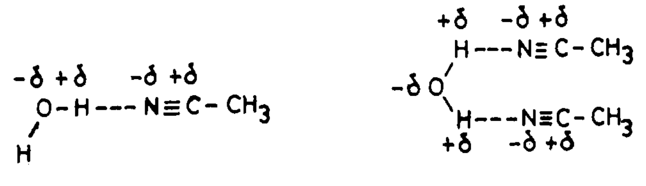

Figure 1. Hydrogen-bonded complexes between water and acetonitrile.

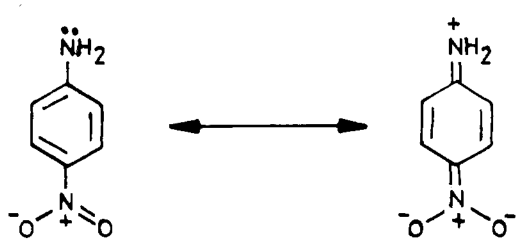

Figure 2. Mesomeric forms of *p*-nitroaniline.

The transfer energies of neutral bases are negative and decrease continuously (Tables I and II) with the addition of organic component, indicating that they are better solvated in the mixed solvents than in water, which can be explained as fol-

Table IV. Thermodynamic Parameters (kJ mol^{-1}) of Various Species Involving mNA in Water-DMF Mixtures at 30 °C (Molal Scale)

wt % DMF	$\Delta G^\circ_{t(B)}$[d]	$\Delta G^\circ_{t(diss)}$[d]	$\Delta G^\circ_{t(HCl)}$[a]	$\Delta G^\circ_{t(Cl^-)}$[b]	$\Delta G^\circ_{t(H^+)}$[c]	$\Delta G^\circ_{t(BH^+)}$	$\Delta G^\circ_{t(BHCl)}$	$\Delta G^\circ_{t(B)} - \Delta G^\circ_{t(BHCl)}$
0	0	0	0	0	0	0	0	0
20	−3.90	−3.95	0.01	2.00 (2.50)	−1.99 (−2.49)	−1.94 (−2.44)	0.06	−3.96
40	−7.40	−6.85	0.43	4.50 (8.00)	−4.07 (−7.57)	−4.62 (−8.12)	−0.12	−7.28
60	−12.02	−10.97	1.96	8.30 (16.00)	−6.34 (−14.04)	−7.39 (−15.09)	0.91	−12.93
80	−14.60	−13.70	7.08	14.00 (23.00)	−6.92 (−15.92)	−7.82 (−16.82)	6.18	−20.78
100	−15.18	−2.73	28.36[e]	35.00 (45.90)	−6.64 (−17.54)	−19.09 (−29.99)	15.91	−31.09

[a] By EMF method ref *20*. [b] By nLJP method, using the relation $\Delta G^\circ_{t(Cl^-)} = \Delta G^\circ_{t(AgCl)} - \Delta G^\circ_{t(Ag^+)}$; the $\Delta G^\circ_{t(AgCl)}$ values were taken from the work of Kundu and Parker (*21*) and $\Delta G^\circ_{t(Ag^+)}$ by nLJP method was taken from the present work. [c] $\Delta G^\circ_{t(H^+)} = \Delta G^\circ_{t(HCl)} - \Delta G^\circ_{t(Cl^-)}$; values in parentheses are based on the TATB method. [d] Accurate to ±0.05 kJ mol^{-1}. [e] Value calculated from ref *23* using the relation $\Delta G^\circ_{t(H^+)} + \Delta G^\circ_{t(Cl^-)} = \Delta G^\circ_{t(HCl)}$.

Table V. Thermodynamic Parameters (kJ mol^{-1}) of Various Species Involving pNA in Water-AN Mixtures at 25 °C (Molal Scale)

wt % AN	$\Delta G^\circ_{t(B)}$[d]	$\Delta G^\circ_{t(diss)}$[d]	$\Delta G^\circ_{t(HCl)}$[a]	$\Delta G^\circ_{t(Cl^-)}$[b]	$\Delta G^\circ_{t(H^+)}$	$\Delta G^\circ_{t(BH^+)}$	$\Delta G^\circ_{t(BHCl)}$	$\Delta G^\circ_{t(B)} - \Delta G^\circ_{t(BHCl)}$
0	0	0	0	0	0	0	0	0
20	−5.56	−3.20	1.25	1.79 (3.86)	−0.54 (−2.61)	−2.90((−4.97)	−1.11	−4.45
40	−10.08	−5.59	3.45	3.68 (7.06)	−0.23 (−3.61)	−4.72 (−8.10)	−1.04	−9.04
60	−12.55	−6.91	7.02	6.40 (9.90)	0.62 (−2.88)	−5.02 (−8.52)	1.38	−13.93
75	−13.68	−7.54	11.91	10.10 (13.60)	1.81 (−1.69)	−4.33 (−7.83)	5.77	−19.45

[a] By EMF method; from ref *20*. [b] By nLJP method. Values in parentheses are based on the TATB method ($\Delta G^\circ_{t(Ag^+)}$ values from ref *21*). [c] $\Delta G^\circ_{t(H^+)} = \Delta G^\circ_{t(HCl)} - \Delta G^\circ_{t(Cl^-)}$. [d] Accurate to ±0.05 kJ mol^{-1}.

Table VI. Thermodynamic Parameters (kJ mol^{-1}) of Various Species Involving pNA in Water-DMF Mixtures at 30 °C (Molal Scale)

wt % DMF	$\Delta G^\circ_{t(B)}$[d]	$\Delta G^\circ_{t(diss)}$[d]	$\Delta G^\circ_{t(HCl)}$[a]	$\Delta G^\circ_{t(Cl^-)}$[b]	$\Delta G^\circ_{t(H^+)}$[c]	$\Delta G^\circ_{t(BH^+)}$	$\Delta G^\circ_{t(BHCl)}$	$\Delta G^\circ_{t(B)} - \Delta G^\circ_{t(BHCl)}$
0	0	0	0	0	0	0	0	0
20	−4.38	−3.66	0.01	2.00 (2.50)	−1.99 (−2.49)	−2.71 (−3.21)	−0.71	−3.67
40	−8.56	−7.26	0.43	4.50 (8.00)	−4.07 (−7.57)	−5.37 (−8.87)	−0.87	−7.69
60	−13.05	−10.85	1.96	8.30 (16.00)	−6.34 (−14.04)	−8.54 (−16.24)	−0.24	−12.81
80	−15.34	−15.90	7.08	14.00 (23.00)	−6.92 (−15.92)	−6.36 (−15.36)	7.64	−22.98
100	−16.41	−4.88	28.36[e]	35.00 (45.90)	−6.64 (−17.54)	−18.17 (−29.07)	16.83	−33.24

[a] By EMF method ref *20*. [b] By nLJP method. [c] $\Delta G^\circ_{t(H^+)} = \Delta G^\circ_{t(HCl)} - \Delta G^\circ_{t(Cl^-)}$; values in parentheses are based on the TATB method. [d] Accurate to ±0.05 kJ mol^{-1}. [e] Values calculated from ref *23* using the relation $\Delta G^\circ_{t(H^+)} + \Delta G^\circ_{t(Cl^-)} = \Delta G^\circ_{t(HCl)}$.

lows. The water-AN mixture is more basic than water itself due to the formation of increased number of monomeric water molecules and their formation of intercomponent hydrogen-bonded complexes with AN molecules (*17*) as shown in Figure 1. In one of the mesomeric forms of pNA, there exists a partial quinonoid structure (Figure 2) such that it gets solvated through the positively charged amino group and the more negative hydroxyl oxygen of monomeric water molecules. Also, the $=N^+H_2$ may interact with the negative end of the dipole of AN. Although solvation of pNA is possible through the interactions of negatively charged atoms of $-NO_2$ group and the positively charged hydrogen atoms of water molecules, the hydrophobic nature of phenyl group hinders this type of interaction. Apart from these interactions, the presence of an aromatic ring suggests the possibility of dispersion interactions with AN molecules. At low compositions of AN, the above-mentioned interactions add together which results in a considerable increase in solubility of pNA. At higher AN compositions, the interactions involving water molecules decrease and the dipole and dispersion interactions due to AN become prominent. Thus a smaller increase in solubility of pNA may be expected in the AN-rich region. A similar argument can be made to explain the observed $\Delta G^\circ_{t(B)}$ variation with solvent composition for pNA in water-DMF mixtures. But the increased basicity of the water-DMF mixtures compared to pure water may be explained as arising due to the formation of H-bonded complexes (Figure 3) of the type $DMF\cdot nH_2O$ which are in general more basic than pure water (*18*, *19*).

The observed $\Delta G^\circ_{t(B)}$ variation with solvent composition for mNA in both water-AN and water-DMF mixtures (since the amino function cannot be in direct conjugation with the nitro function) can be explained by considering the structure b of Figure 4 to interact with the basic sites of the solvent mixtures, all the other arguments being similar to the one given for pNA in water-AN mixtures.

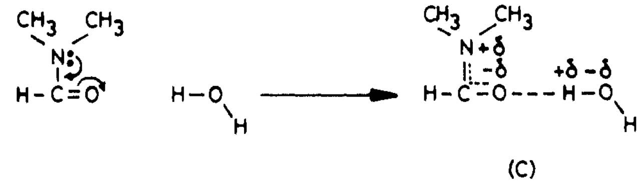

Figure 3. Hydrogen-bonded complexes between water and *N*,*N*-DMF.

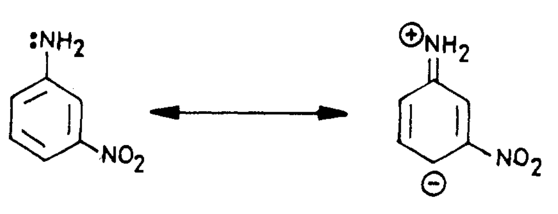

Figure 4. Mesomeric forms of *m*-nitroaniline.

The negative and continuously decreasing $\Delta G^\circ_{t(H^+)}$ values for water-AN (upto 40 wt % AN) and water-DMF mixtures (Tables III-VI), on the basis of both nLJP and TATB methods, may be attributed to the enhanced basicity of the solvent mixtures as pointed out already.

The $\Delta G^\circ_{t(BH^+)}$ for both $pNAH^+$ and $mNAH^+$ ions in water-AN and water-DMF mixtures (Tables III-VI) is negative throughout the range of solvent compositions and generally decreases continuously with the addition of the organic solvent component (both on nLJP and TATB methods) although there is a slight increase; i.e., the value becomes less negative at 75 wt % AN and 80 wt % DMF for $pNAH^+$ ion in these mixtures, respectively. Thus these ions are better stabilized in the mixed solvents than in water which can be explained on the basis of the increased basicity of the solvent mixture than pure water. In both $pNAH^+$ and $mNAH^+$, the $-NH_3^+$ group will be solvated by the negative end of the oxygen of $-OH$ group in the mixed solvent or even by the negative end of the AN dipole or DMF dipole (see the intercomponent H-bonded structures of water with AN and DMF in Figures 1 and 3). Further, the solvation of $pNAH^+$ and $mNAH^+$ can also occur through the negatively charged atoms of the $-NO_2$ group and the positively charged H atoms of water molecules. At higher compositions of the dipolar aprotic solvent components, the possibility of dispersion interactions can lead to the large negative values of $\Delta G^\circ_{t(BH^+)}$.

The $\Delta G^\circ_{t(BHCl)}$ values for mNA (Table III) and pNA (Table V) in water–AN mixtures are negative and decrease initially with the addition of AN upto 30 and 20 wt % AN, respectively, and thereafter increase to positive values till pure AN. In water–DMF mixtures, the $\Delta G^\circ_{t(BHCl)}$ values for both mNA and pNA are very nearly equal to zero upto about 60 wt % DMF (Tables IV and VI) and thereafter are positive and increase continuously with the addition of DMF. The very low values of $\Delta G^\circ_{t(BHCl)}$ upto 60 wt % organic solvent component in both water–AN and water–DMF mixtures can be explained as arising from the nearly equal and opposite values of $\Delta G^\circ_{t(BH^+)}$ (which is negative throughout) and $\Delta G^\circ_{t(Cl^-)}$ (which is positive throughout) upto this solvent composition. But beyond 60 wt % organic solvent component, the magnitudes of $\Delta G^\circ_{t(Cl^-)}$ are very high compared to those of $\Delta G^\circ_{t(BH^+)}$ and they overshadow the decrease in $\Delta G^\circ_{t(BH^+)}$ which results in large positive values of $\Delta G^\circ_{t(BHCl)}$ after this composition.

The increasing positive values of $\Delta G^\circ_{t(Cl^-)}$ in both the solvent mixtures can be explained as arising from the decreasing H-bonding availability for Cl^- ions in water–DMF and water–AN mixtures compared to that in pure water. This is because both DMF and AN form H-bonded complexes and hence there will be a competition for water molecules by both Cl^- and the organic solvent component.

Registry No. mNA, 99-09-2; pNA, 100-01-6; AN, 75-05-8; DMF, 68-12-2.

Literature Cited

(1) Bates, R. G. *J. Electroanal. Chem.* **1960**, *29*, 209.
(2) Rao, V. S.; Kalidas, C. *Indian J. Chem.* **1977**, *15A*, 118.
(3) Kundu, K. K.; De, A. L.; Das, M. N. *J. Chem. Soc., Dalton Trans.* **1972**, 386.
(4) Bates, R. G. *Hydrogen Bonded Solvent Systems*; Covington, A. K., Jones, P., Eds.; Taylor and Francis: London, 1968; p 49.
(5) Sivaprasad, P.; Kalidas, C. *Monatsh. Chem.* **1981**, *112*, 1369.
(6) Kalidas, C.; Janardhanan, S. *Indian J. Chem.* **1983**, *22A*, 17.
(7) Venkateswara Sastry, V. Ph.D. Dissertation, Indian Institute of Technology, Madras, 1983.
(8) Subramanian, S.; Rao, S. C. A. V. S. S.; Kalidas, C. *Indian J. Chem.* **1981**, *20A*, 723.
(9) Giridhar, V. V.; Kalidas, C. *Proc. Indian Acad. Sci.* (*Chem. Sci.*) **1984**, *93*, 796.
(10) Vogel, A. I. *Practical Organic Chemistry*; ELBS and Longman: London, 1978; p 662, 686.
(11) Kalidas, C.; Palit, S. R. *J. Chem. Soc.* **1961**, 3998.
(12) Paul, M. A.; Long, F. A. *Chem. Rev.* **1957**, *57*, 1.
(13) El-Harakany, A. A.; Sabet, V. M.; Sadek, H. *Z. Phys. Chem. N. F.* **1975**, *97*, 225.
(14) Robinson, R. A. *J. Res. Natl. Bur. Stand A.* **1970**, *74*, 495.
(15) Bolton, P. D.; Hall, F. M. *Aust. J. Chem.* **1968**, *21*, 939.
(16) Biggs, A. I. *J. Chem. Soc.* **1961**, 2572.
(17) Das, K.; Das, A. K.; Kundu, K. K. *Electrochim. Acta* **1981**, *26*, 471.
(18) Das, K.; Bose, K.; Kundu, K. K. *Electrochim. Acta* **1981**, *26*, 481.
(19) Singh, D.; Lal Bahadur; Ramanamurthy, M. V. *J. Solution Chem.* **1977**, *6*, 703.
(20) Smith, R.; Massart, D. L.; Juillard, J.; Morel, J. P. *Electrochim. Acta* **1976**, *21*, 431.
(21) Kundu, K. K.; Parker, A. J. *J. Solution Chem.* **1982**, *11*, 847.
(22) Cox, B. G.; Parker, A. J.; Waghorne, W. E. *J. Phys. Chem.* **1974**, *78*, 1731.
(23) Kolthoff, I. M.; Chantooni (Jr), M. K. *J. Phys. Chem.* **1972**, *76*, 2024.

Received for review January 21, 1986. Revised July 23, 1986. Accepted November 6, 1986. The financial assistance from CSIR, New Delhi, and the Indian Institute of Technology, Madras, is gratefully acknowledged.